International Journal of Mechanical and Electrical Engineering
ISSN: 3005-9615 (Print), ISSN: 3005-7132 (Online) | Volume 2, Number 2, Year 2024
DOI: https://doi.org/10.62051/ijmee.v2n2.13
Journal homepage: https://wepub.org/index.php/IJMEE/index

Research and Characteristic Analysis of A New Type of Dual Winding Electromagnetic Brake

Tongliang Liu *, Shida Sun

College of Electrical Engineering, Henan Polytechnic University, Jiaozuo, China
* Corresponding Author: Tongliang Liu

ABSTRACT

Taking the electromagnetic brake as the research object, a new structure of double-winding electromagnetic brake is proposed in view of the serious temperature rise phenomenon of traditional single-winding electromagnetic brake, the high requirement of insulation level and the obvious decrease of electromagnetic force. The equivalent magnetic circuit method is used to analyze and calculate the magnetic field, and the simulation model of the new brake is constructed, and the influence of different parameters on the braking characteristics of the double-winding electromagnetic brake is analyzed by the single-variable method, and the influence curves of each parameter on the electromagnetic force and response time are obtained. At the same time, the magnetic-thermal coupling analysis of the double-winding electromagnetic brake is carried out, and the results show that the total ampere-turns and power of the double-winding electromagnetic brake decreases by 15.3% in the same proportion, the rated electromagnetic force decreases by 22.9%, the release time grows by 23.7%, and the closure time is shortened by 14.6%.

KEYWORDS

Double Winding; Equivalent Magnetic Circuit Method; Braking Characteristics; Temperature Field Model.

1. INTRODUCTION

Electromagnetic brakes have the advantages of simple structure, convenient control and installation, and electromagnetic power loss brake is a widely used type of electromagnetic brake. Electromagnetic power loss brake (power on release, power off braking) is a braking device that relies on the mutual friction between the friction disc and the brake disc to achieve the desired braking effect[2]. Electromagnetic powered brakes can meet the requirements of the high-speed development of modern industry for the smoothness, safety, and reliability of production processes. They are widely used in industrial automation, aerospace, heavy industry, precision machinery, and other fields[3],[4].

When the motor transmission device requires long-term continuous operation, the electromagnetic power loss brake must be powered on for a long time to work. The brake coil heats up due to long-term power on. When the electromagnetic brake does not have a good heat dissipation device, the coil will age due to long-term heating, ultimately causing a turn to turn short circuit fault in the brake coil. In order to improve the stability of electromagnetic brakes and reduce the impact of temperature rise, this paper proposes a new type of electromagnetic brake with dual windings. The equivalent magnetic circuit method was used to calculate the main magnetic flux of the new electromagnetic brake, and the effects of structural size, air gap length, and coil turns on the brake performance were

analyzed[5],[6]. A magneto-thermal coupling analysis of a double-winding electromagnetic brake (DWEB) was carried out to investigate the effect of temperature rise on the brake performance.

2. DESIGN OF A NEW ELECTROMAGNETIC BRAKE

2.1. Main Technical Parameters of DWEB

The structure of DWEB is shown in Fig.1, and its working principle is the same as that of single winding electromagnetic brake (SWEB). When the brake is powered off, the force generated by the spring acts on the armature, causing the friction disc to tightly clamp between the armature and the rotor, thereby generating a braking torque. At this point, a gap will be created between the armature and the stator[7]. When it is necessary to release the brake, the coil is energized, and the generated magnetic field attracts the armature to move towards the stator. When the armature moves, the spring is compressed, and the friction disc component is released, releasing the brake. The inner and outer coils are connected in parallel in the same direction. After parallel connection, the total impedance of the circuit decreases, the power increases, the power density increases, and the electromagnetic force generated by the brake is greater. The main technical parameters of the DWEB are shown in Table 1.

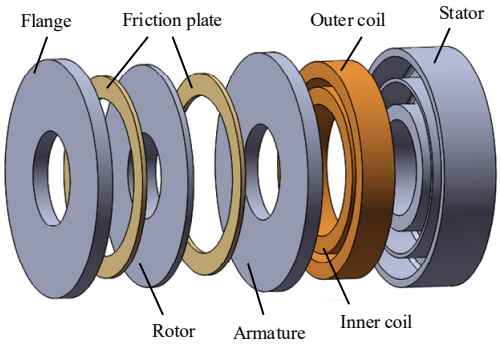

Fig 1. Structure diagram of DWEB

Table 1. Main technical parameters of DWEB

Parameter	Value
Rated voltage/V	170
Initial air gap/mm	0.5
Rated torque/N·m	400
Inner diameter of friction plate/mm	198
Outer diameter of friction plat/mm	254

2.2. Rated Electromagnetic Force

As shown in Fig.1, the friction plate of the DWEB has two contact surfaces simultaneously to provide friction. Both contact surfaces are circular, and the rated spring force can be obtained from equation (1) as:

$$F_{\mathrm{T}} = \frac{3f(D_2^2 - D_1^2)T}{2\mu(D_2^3 - D_1^3)} = 7043\mathrm{N}\,. \tag{1}$$

Where T is the rated braking torque, N·m; D_1 and D_2 are the inner and outer diameters of the friction plate, m; μ is the friction coefficient of the friction plate, taken as 0.3; F is the safety factor, taken as 1.2.

According to equation (2), the electromagnetic force required for the electromagnetic brake is:

$$F_{EM} = F_{\mathrm{T}} \times f^{'} = 8452\mathrm{N}\,. \tag{2}$$

Where f' is the safety factor, taken as 1.2.

3. ELECTROMAGNETIC ANALYSIS OF DWEB

3.1. Magnetic Circuit Analysis

The inner and outer coils of the DWEB adopt a parallel structure in the same direction, which can reduce the equivalent resistance of the windings. Compared to the SWEB, it has greater electromagnetic force and power density under the same volume. When the electromagnetic brake operates, it can be regarded as an E-type electromagnet. When the power is supplied, the electromagnetic coil inside the stator generates current simultaneously, which will generate electromagnetic force on the inner yoke of the stator. The magnetic flux passes through the bottom of the stator to the outer yoke of the stator, then passes through the air gap to the armature, and then returns to the inner yoke of the stator through the air gap to form a closed circuit. Due to the opposite direction of magnetic flux generated by the inner and outer coils on the yoke on the middle side of the stator, the total magnetic flux on the yoke on the middle side of the stator is small, resulting in a smaller electromagnetic force. The direction of magnetic flux is related to the number of ampere turns of the coil and the structure of the iron core[8]. This article uses the segmented magnetic circuit method to analyze the main magnetic flux of the brake, as shown in Fig.2. The influence of magnetic leakage is ignored in the calculation process.

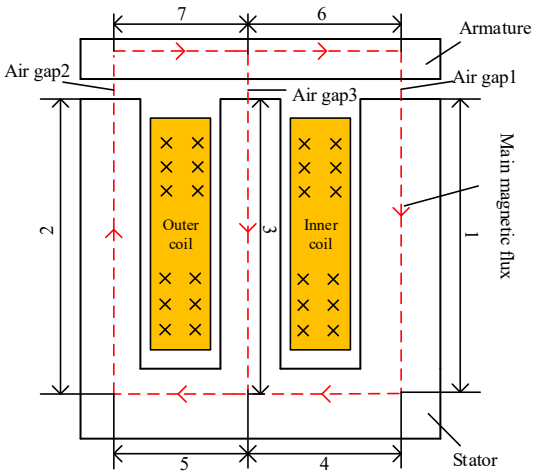

Fig 2. Main magnetic circuit diagram of DWEB

The equivalent magnetic circuit of the DWEB is shown in Fig.3, where N represents the number of turns of the inner and outer coils, I_1 and I_2 represent the current of the inner and outer coils, the stator reluctance is equivalent to R_1, R_2, R_3, R_4, R_5, the armature reluctance is equivalent to R_6, R_7, and the air gap reluctance is equivalent to R_{ag1}, R_{ag2}, and R_{ag3}.

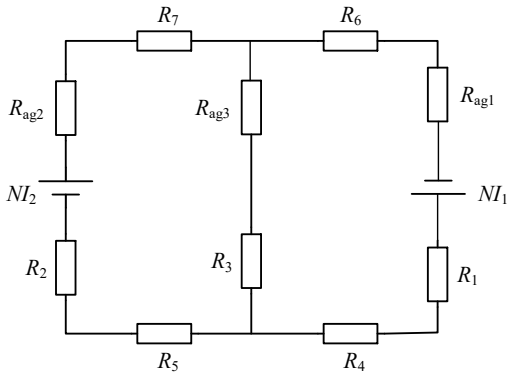

Fig 3. Equivalent magnetic circuit diagram of DWEB

As shown in Fig.3, the total electromagnetic force of the DWEB is jointly generated by the inner and outer coils. The total magnetic flux Φ is composed of air gap fluxes Φ_1, Φ_2, and Φ_3 corresponding to the working air gaps. The magnetic circuit equation obtained from Kirchhoff's first law and Kirchhoff's second law is shown in equation (3):

$$\begin{cases} NI_1 = \Phi_1\left(R_1 + R_4 + R_6 + R_{\text{ag1}}\right) + \Phi_3\left(R_3 + R_{\text{ag3}}\right) \\ NI_2 = \Phi_2\left(R_2 + R_5 + R_7 + R_{\text{ag2}}\right) - \Phi_3\left(R_3 + R_{\text{ag3}}\right) \\ \Phi_3 = \Phi_1 - \Phi_2 \end{cases} \tag{3}$$

Air gap reluctance

The working air gaps section of the electromagnetic brake is a circular ring type, and its reluctance is shown in equation (4):

$$R_{\text{ag}i} = \frac{\delta}{\mu_0 S_i}\left(i = 1, 2, 3\right) \tag{4}$$

Where δ Is the maximum length of the working air gaps; μ_0 is the air permeability (approximately equal to the vacuum permeability, μ_0=4π×10^{-7}H/m); S_i is the cross-sectional area of each working air gaps.

Stator side yoke reluctance

The stator side yoke is divided into three parts: the inner yoke, the outer yoke, and the middle yoke, with a cross-sectional area equal to the corresponding working air gaps cross-sectional area. The reluctance is shown in equation (5):

$$R_i = \frac{L_i}{\mu_1 S_i}(i = 1, 2, 3) \tag{5}$$

Where L_i is the height of the yoke on each section; μ_1 is the saturation permeability of ferromagnetic materials. Due to the use of low carbon steel as the ferromagnetic material for the armature and stator, the permeability of the ferromagnetic material should be calculated based on its magnetic flux saturation. Therefore, it is approximately assumed that the permeability of each part is the same. According to the magnetization curve of low-carbon steel, the saturation magnetic induction intensity is about 2.0T, and the relative permeability at saturation is generally taken as μ_r=50-100.

Stator bottom yoke reluctance

The yoke at the bottom of the stator is a cylinder, and the magnetic flux direction is in the radial direction, as shown in equations (6) and (7):

$$R_4 = \frac{L_4}{2\pi r_4 \mu_1 m} \tag{6}$$

$$R_5 = \frac{L_5}{2\pi r_5 \mu_1 m} \tag{7}$$

Where L_4 and L_5 are the effective lengths of two magnetic circuits; R_4 and R_5 are the average radii of the two magnetic circuits; m is the height of the bottom of the stator.

Armature reluctance

The calculation method of armature reluctance is similar to that of stator bottom yoke reluctance, as shown in equations (8) and (9):

$$R_6 = \frac{L_6}{2\pi r_6 \mu_1 n} \tag{8}$$

$$R_7 = \frac{L_7}{2\pi r_7 \mu_1 n} \tag{9}$$

Where L_6 and L_7 are the effective lengths of two magnetic circuits; R_6 and R_7 are the average radii of the two magnetic circuits; n is the thickness of the armature.

3.2. Magnetic Density Calculation

The electromagnetic force of an electromagnetic brake is generated by the working air gaps, and its calculation equation is shown in equations (10) and (11):

$$\begin{aligned} F_{EM} &= F_1 + F_2 + F_3 \\ &= \frac{B_{1av}^2 S_1 + B_{2av}^2 S_2 + B_{3av}^2 S_3}{2\mu_0} \end{aligned} \tag{10}$$

$$B_{iav} = \frac{\Phi_i}{S_i} (i = 1,2,3) \tag{11}$$

Where F_1, F_2, and F_3 respectively represent the electromagnetic forces generated by the three working air gaps; B_{1av}, B_{2av}, and B_{3av} are the average magnetic flux densities of the three working air gaps.

The main parameters of the DWEB preliminarily selected in this article are shown in Table 2.

Table 2. Main structural parameters of DWEB

Parameter	Value
Spring force/N	7043
Number of turns	2*5000
Maximum air gap/mm	1.5
Inner diameter of stator/mm	120
Outer diameter of stator/mm	300
Height of stator/mm	70
Height of stator bottom/mm	20
Thickness of armature/mm	20

4. CHARACTERISTIC ANALYSIS OF DWEB

The rated electromagnetic suction that can be generated at the maximum air gap when an electromagnetic brake is energized, the release time required from coil energization to complete release of the armature, and the closing time required from coil power outage to complete closure of the armature are important standards for measuring brake performance[9]. The magnitude of the rated electromagnetic force directly affects the selection of spring force, reflecting the selection range of brake braking torque; The release time and closing time reflect the sensitivity of the brake. This article establishes a simulation model of the DWEB, and uses the single variable method to analyze the influence of different parameters on the electromagnetic characteristics of the DWEB. The influence curves of each parameter on the electromagnetic force and response time are obtained. By optimizing the parameters of the DWEB through simulation results, the optimal results are obtained.

4.1. The Influence of Maximum Air Gap Length On Braking Characteristics

The selection of the maximum working air gap length is closely related to the service life of the brake. Due to the wear of the brake friction plates during the braking process, the friction plates gradually become thinner, the working air gap increases, and the electromagnetic force decreases. Therefore, attention should be paid to adjusting the air gap length of the brake during use.

The curve of the electromagnetic force generated by the DWEB with different air gap lengths over time when energized is shown in Fig.4(a), and the release time required from coil energization to

complete release of the armature is shown in Fig.4(b). As the length of the air gap increases, the reluctance of the air gap continues to increase, and the electromagnetic force generated by the brake at the maximum air gap decreases, resulting in an increasing release time. According to equation (2), in order to meet the safety factor, the electromagnetic suction required for the brake at the maximum air gap is 8452N. When the maximum air gap length is 1.75mm, the electromagnetic force generated by the brake does not meet the requirements of the safety factor. Taking into account factors such as electromagnetic suction, release time, and service life, the maximum working air gap selected in this article is 1.25 mm.

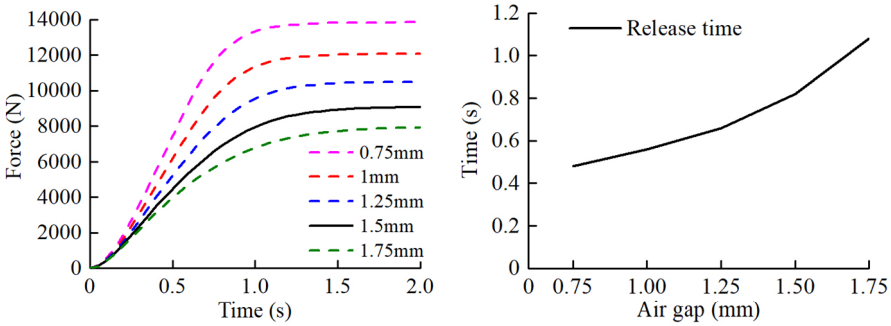

(a) Electromagnetic force (b) Release time

Fig 4. Effect of maximum air gap length on brake performance

4.2. The Influence of Iron Core Parameters On Braking Characteristics

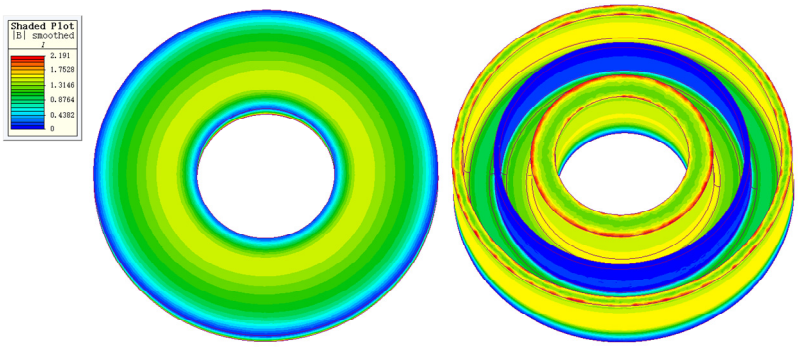

(a) Armature (b) Stator

Fig 5. Magnetic density cloud diagram of DWEB

From equation (3), it can be seen that the inner and outer ring coils of the DWEB generate opposite magnetic flux directions on the middle side yoke of the stator. Therefore, the total magnetic flux on the middle side yoke is relatively small, which has little impact on the electromagnetic force of the DWEB. Fig.5 shows the magnetic density cloud diagram of the DWEB. It can be seen from Fig.5 that the simulation results are consistent with the previous analysis results, verifying the rationality of the previous mathematical model. Due to the leakage of magnetic flux generated during the operation of the brake, the selection of the area of the inner and outer yoke of the brake is one of the important parameters for optimizing the electromagnetic performance of the brake. Now keeping the total area of the inner and outer yokes unchanged and changing the area ratio of the inner and outer yokes, the curve of the electromagnetic force at the maximum air gap of the DWEB with time is shown in Fig.6(a), and the effect of the area ratio of the inner and outer yokes on the response time is shown in Fig.6(b). As the area of the inner yoke increases, the maximum electromagnetic force generated by the DWEB first increases and then decreases, reaching its peak when the area ratio of the inner and outer yoke is 1.1:1; The release time first decreases and then increases with the increase of the area ratio of the inner and outer yokes, while the closing time increases with the increase of the

area ratio of the inner and outer yokes, and the increasing trend gradually slows down. Therefore, after comprehensive consideration, the final selected area ratio of the inner and outer yoke is 1.1:1.

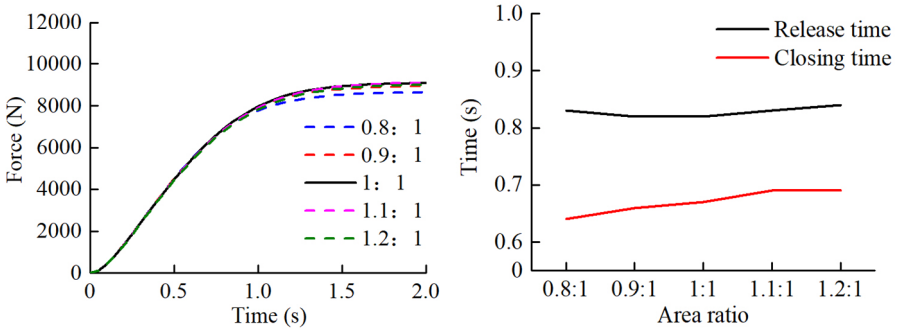

(a) Electromagnetic force (b) Response time

Fig 6. Effect of inner and outer yoke area ratio on brake performance

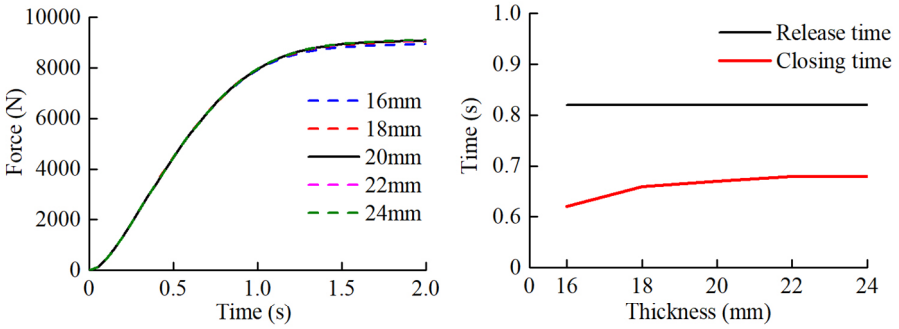

(a) Electromagnetic force (b) Response time

Fig 7. Effect of armature thickness on brake performance

The influence of armature thickness on the electromagnetic characteristics of DWEB is shown in Fig.7. As the thickness of the armature increases, the reluctance of the armature gradually decreases, and the electromagnetic force generated by the DWEB at the maximum air gap gradually increases, and the increasing trend gradually slows down. When energized, the release time remains basically unchanged as the thickness of the armature increases; When power is cut off, the thicker the armature, the longer the closing time of the brake. In order to reduce the response time of the DWEB and improve the sensitivity of the brake, after comprehensive consideration, the final selected armature thickness is 16mm.

4.3. The Influence of Coil Turns On Braking Characteristics

The influence of coil turns on the electromagnetic characteristics of the DWEB is shown in Fig.8. According to the electromagnetic force calculation equation, it is known that the electromagnetic force is related to the total ampere turns of the brake. As the number of coil turns increases, the coil resistance linearly increases, the excitation current decreases, the total ampere turns decrease, and the maximum electromagnetic force generated by the brake decreases; however, due to the increase in turns, the inductance of the coil will also increase, resulting in a slower charging and discharging speed of the coil and an increase in the response time of the brake; the decrease in excitation current will cause a decrease in brake power, thereby reducing brake losses. Taking into account factors such as electromagnetic force, response time, and power, the final selection of coil turns is 2*4500.

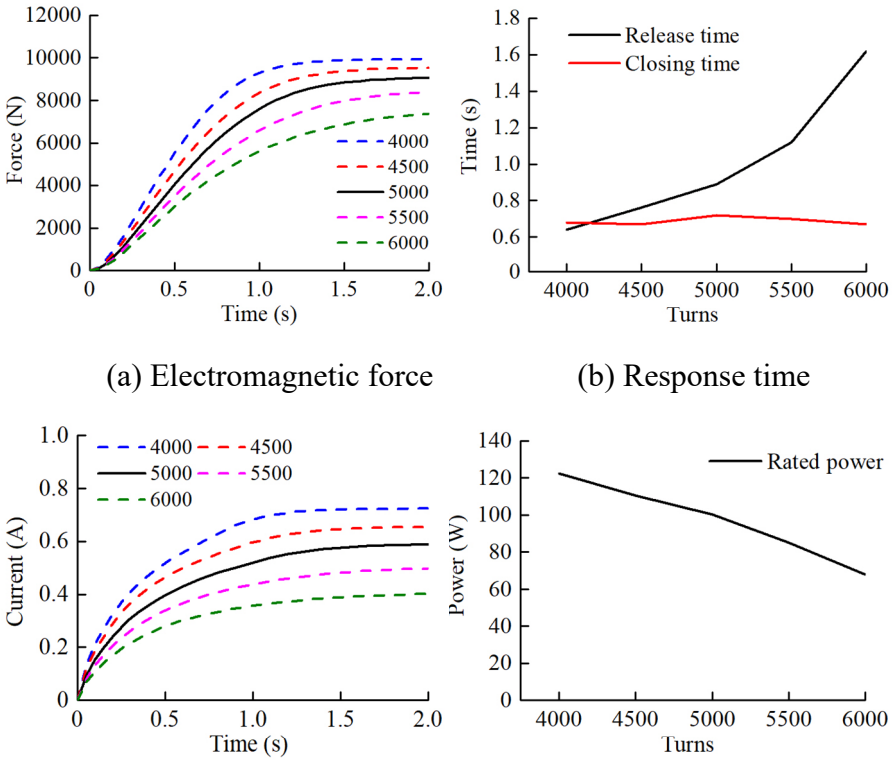

(a) Electromagnetic force (b) Response time

(c) Current (d) Power

Fig 8. Effect of coil turns on brake performance

Taking into account the effects of air gap length, side yoke area, armature thickness, and coil turns on the electromagnetic performance of the DWEB, the main structural parameters of the DWEB selected in this article are shown in Table 3.

Table 3. Main parameters of DWEB

Parameter	Value
Spring force/N	7043
Number of turns	2*4500
Maximum air gap/mm	1.25
Inner diameter of stator/mm	117.5
Outer diameter of stator/mm	298.5
Height of stator/mm	70
Height of stator bottom/mm	20
Thickness of armature/mm	16

5. TEMPERATURE FIELD ANALYSIS

Electromagnetic powered brakes generally operate for a long period of time, therefore, it is necessary to consider the impact of temperature rise in the coil on brake performance. An increase in coil temperature will lead to an increase in resistance, a decrease in excitation current, a decrease in ampere turns, insufficient electromagnetic suction, and ultimately the inability to unlock the brake, affecting its working performance. At the same time, excessive temperature will also put forward higher requirements for the insulation performance of the brake, increasing production costs[10].

The temperature field analysis results of the DWEB is shown in Fig.9. The heat transfer of the brake starts from the electromagnetic coil and is conducted outward in a decreasing temperature gradient. Due to the small resistance, high current, and small volume of the inner coil, the power and thermal load of the inner coil are higher, and its temperature is higher than that of the outer coil. The maximum

temperature of the inner coil is 106.2℃, the maximum temperature of the outer coil is 82.8℃, and the minimum temperature of the stator surface is 54.5℃.

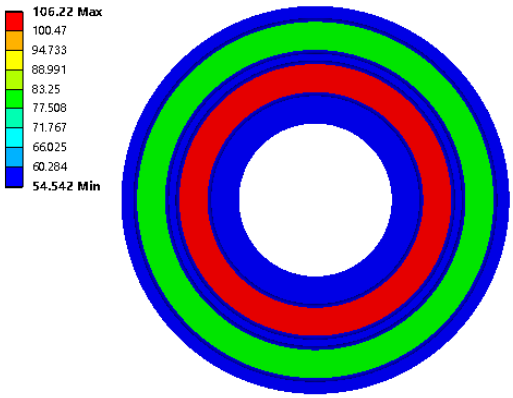

Fig 9. Temperature distribution diagram of DWEB

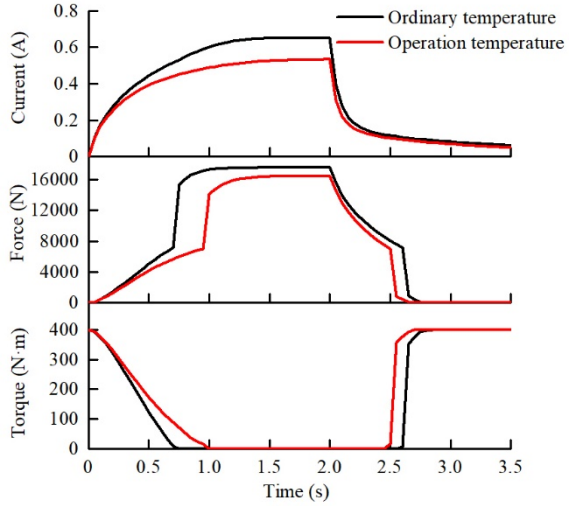

Fig 10. Dynamic characteristic curves of DWEB at different temperatures

Table 4. Performance comparison of DWEB at different temperatures

	Normal temperature	Working temperature
Rated current/A	0.65	0.53
Total ampere turns	2925	2385
Power/W	110.5	90.1
Rated electromagnetic force/N	10016	8495
Release time/s	0.68	0.95
Closing time/s	0.62	0.50

Under different temperatures, the dynamic characteristic curve of the double-winding electromagnetic brake is shown in Fig.10. When the double-winding electromagnetic brake is in a long-time operating state, the performance changes after the inner and outer coil temperatures increase are shown in Table 4. From Table 4, it can be seen that when the coil temperature rises, the coil resistance increases and the current decreases, resulting in the total ampere-turns and power decreasing by 18.5% in the same proportion, and the rated electromagnetic force decreasing by 15.2%;

and the influence on the corresponding time of the brake is even larger, with the release time increasing by 39.7% and the closing time shortening by 19.3%.

6. SUMMARIZE

In response to the serious temperature rise and significant decrease in electromagnetic suction of traditional single winding electromagnetic power loss brakes, this paper proposes a new structure of dual winding electromagnetic power loss brakes. Taking a new type of brake as the research object, the equivalent magnetic circuit method was used to analyze and calculate its magnetic field. A simulation model of the new type of brake was built, and the single variable method was used to analyze the influence of different parameters on the electromagnetic characteristics of the new type of brake. The influence curves of each parameter on the electromagnetic force and response time were obtained.

Joint simulation of electromagnetic and temperature fields was conducted on the new DWEB, and the results showed that: the total ampere-turns and power decreasing by 18.5% in the same proportion, and the rated electromagnetic force decreasing by 15.2%; and the influence on the corresponding time of the brake is even larger, with the release time increasing by 39.7% and the closing time shortening by 19.3%.

REFERENCES

[1] Li Xiaokun, Dong Fang, Xu Baoyu. Driver Architecture Design and Performance Analysis of the Normal Closed Electromagnetic Brake[J]. Journal of Astronautic Metrology and Measurement,2019,39(05):59-64.

[2] Song Zhenmin, Su Wei, Li Yu, et al. Design Technology of Permanent Magnet Loss Brake Based on ANSYS[J]. Small & Special Electrical Machines,2021,49(09):28-32.

[3] Yang Shuyi, Zhao Kangkang, Zhang Hongtai,et al. Braking Stability Analysis of Wind Turbines Yaw Brake[J].Acta Energiae Solaris Sinica,2023,44(01):188-195.

[4] Zhang Bo, Wang Huiling, Huang Lindi, et al. Design and Simulation of Electromagnetic Loss Brake Based on the Ansys[J]. Micromotors, 2015,48(02):21-25+31.

[5] Liu Chao, Zhang Qiang, Su Jufang, et al. Calculation and Analysis of Solenoid Electromagnet for Spring Operating Mechanism[J]. High Voltage Apparatus,2020, 56(12):91-96.

[6] Liu Chao, Zhao Weitao, Zhang Qiang,et al. Simulation and Optimization for Mechanical Characteristics of Spring Operating Mechanism in Vacuum Circuit Breaker[J]. High Voltage Apparatus, 2019,55(08):65-71.

[7] Meng Zhoutian, Dan Shuheng. Structural Optimization Design of Electromagnetic Repulsive Mechanism with Finite Element Method and Neural Network Method[J]. High Voltage Apparatus,2021,57(06):196-202.

[8] Wang Lina, Liu Yang, Zhao Zhizhong. Structural Design and Magnetic Field Analysis of Bidirectional Coil-plate Electromagnetic Repulsion Mechanism[J]. Power System Technology,2023,47(09):3924-3934.

[9] Wu Jin, Zhuang Jinwu, Wang Chen, et al. Simplification and Solution of the Mathematical Model to Electromagnetic Repulsion Mechanism [J]. Proceedings of the CSEE,2013,33(24):175-182+25.

[10] Wang Yuan, Li Yulong, Li Junxia. Thermal Mechanical Coupling Analysis and Temperature Test of Disc Brake[J]. Coal Technology, 2019,38(01):145-149.